Journal of Photopolymer Science and Technology
Volume23,Number1(2010)101 – 108 ©2010CPST

Visible Light Photoinitiating Systems: Toward a Good Control of the Photopolymerization Efficiency

A. Ibrahim, C. Ley, O. I. Tarzi, J. P. Fouassier, X. Allonas*

Department of Photochemistry, CNRS, University of Haute Alsace, ENSCMu, 3 rue Alfred Werner, 68093 Mulhouse Cedex – France.
xavier.allonas@uha.fr

This paper discusses the photochemistry of three-component photoinitiating systems (3K-PIS) for free radical photopolymerization and the efforts made during the last decades to propose efficient systems applied to the laser imaging area. A special focus is devoted to a new 3K-PIS working in the green region. It is based on a pyrromethene dye which is reduced or oxidized by a coinitiator. A third redox component is used that leads to the recovery of the initial dye and the formation of additional initiating species, preventing a fast photobleaching of the dye. The beneficial effect on the photopolymerization rates and the final monomer conversion is clearly noticed. Laser flash photolysis was used to understand the reaction mechanisms, and detailed photopolymerization kinetics allow the study of polymeric network formation.

Keywords: photoinitiating system, laser spectroscopy, photopolymerization.

1. Introduction

Photopolymerization represents nowadays a widely used technology in very different fields of application ranging from the coating industry to microelectronics, graphic arts or optics. [1-4]

Many different photoinitiating systems are commercially available covering a wide range of applications using mainly UV irradiation sources. However, there is still a lack of efficient and usable photoinitiating systems for some applications that require visible light irradiation. By example, computer-to-plate technology, laser direct imaging, holography... are such technologies for which there is a real need of photoinitiating systems working in the visible region under narrow line light sources such as lasers. Visible-light photoinitiating systems have been always considered as quite challenging. Different methods have been proposed and among them the use of additional redox additives, leading to the so-called three-component photoinitiating systems was pointed out. [5] However, the exact mechanisms taking place in the bulk resin have never been clearly elucidated, and their relative efficiency is still largely underestimated.

In this paper, a pyrromethene dye (1, 3, 5, 7, 8 - pentamethyl - 2, 6 - diethyl -pyrromethene - difluoroborate complex, EMP) was used together with a reductant coinitiator (N-Phenylglycine, NPG) and oxidant coinitiator (2-(4- methoxyphenyl)- 4,6- bis- (trichloro-methyl)- 1,3,5 -triazine, TA), as depicted in Scheme 1. The initial mechanism of reaction depends on the relative concentration of the oxidant and the reductant. After a first initial excited state quenching, secondary reactions involving the second redox additive take place, leading to beneficial effects such as dye ground state recovery and formation of additional

Received April 24, 2010
Accepted May 21, 2010

initiating species. The efficiency of these processes is deeply investigated, and the effect on the polymeric network formation is detailed.

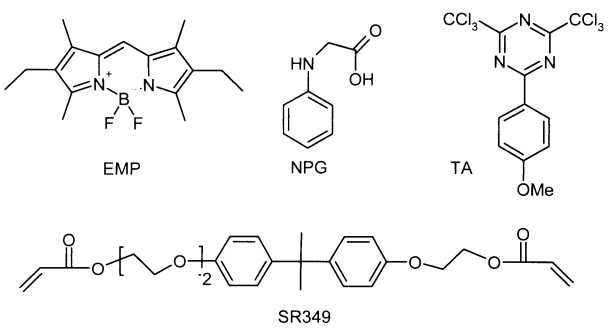

Scheme 1. Compounds used in this study.

2. Experimental

2.1. Materials

1, 3, 5, 7, 8 - pentamethyl - 2, 6 - diethyl -pyrromethene - difluoroborate complex (EMP) was purchased from Exciton. N-Phenylglycine (NPG) was obtained from Aldrich. 2-(4-methoxyphenyl)-4,6-bis(trichloromethyl)-1,3, 5-triazine (TA) was a gift from Produits Chimiques Auxiliaires et de Synthèses (Longjumeau, France). Ethoxylated bisphenol A diacrylate (SR 349) was a gift from Cray Valley, France.

2.2. Photopolymerization experiments

Photopolymerizable samples were prepared using an ethoxylated bisphenol A diacrylate (SR 349, Sartomer Cray Valley) as monomer and the photoinitiating system using 0.1 weight percent of dye. Each sample is sealed between two polypropylene foils. The sample thickness is about 20 µm. Table 1 shows the composition of the different runs. The photopolymerization kinetic was followed by real time FTIR spectroscopy (Vertex 70, Bruker) as described elsewhere [6-7]. Rates of polymerization Rp are easily calculated from the monomer conversion C(%) vs. time curves and from the initial acrylate double bond concentration $[M_0]$ according to :

$$Rp = \frac{[M_0]}{100}\frac{dC(\%)}{dt} \qquad (1)$$

In the following the value $(Rp/[M]_0)x\ 100$ will be reported for the polymerization rates and noted by Rp in the different tables. A diode laser emitting at 532 nm was used to irradiate the sample within the RT-FTIR chamber.

The nanosecond transient absorption setup is based on a Nd:Yag laser (Powerlite 9010, Continuum) operating at 10 Hz. This laser delivers nanosecond pulses at 532 nm with an energy about 5-8 mJ. The transient absorption analyzing system (LP900, Edinburgh Instruments) consists in a 450W pulsed xenon arc lamp, a Czerny–Turner monochromator, a fast photomultiplier and a transient digitizer. This experimental setup is characterized by an instrumental response of about 7 ns [8-9].

3. Three component photoinitiating systems

Most of the systems commercially available for free radical photopolymerization are based on Type I or Type II photoinitiators which generally can not be irradiated in the visible region of the electromagnetic spectrum. Only few dyes absorbing in the visible region can react directly as Type II photoinitiators. Methylene Blue is well known to react with amine from its triplet state thereby initiating the polymerization. Very good efficiencies have been also reported using Thionine, Rose Bengal, Eosin Y, Erythrosin, Riboflavin as photoinitiators and coinitiators such as amines, sulfinates, carboxylates [1-4, 10-12]. In the case of amine as coinitiator, the reaction involves an hydrogen abstraction from the amine to form the semi-reduced form of the dye. Side-reactions can occur that involve back electron transfer processes, oxygen inhibition... These systems are able to shift the spectral sensitivity of photopolymerisable resins up to the red region of the visible spectrum.

However, even if some dyes can be used to red-shift the absorption spectrum, these photoinitiating systems have very limited potential application due to their relatively low efficiency. Indeed, the conversion of the monomer was generally limited. Most of the industrial applications require conversions of more than 60%, a goal that is difficult to achieve with conventional dye / coinitiator photoinitiating systems. In addition, dark reactions take place leading to poor shelf life and consequently two-component dye / coinitiator photoinitiating systems were not developed so far.

Then, other photoinitiating systems were developed using a photosensitizer (PS) that absorbs the visible light and lead to a photochemical reaction with a photoinitiator, either by electron or energy transfer. A well known family of such photoinitiators that

could be easily sensitized concerns the derivatives of hexaarylbisimidazoles, and particularly the chloro-derivative, introduced in the 70s [13]. Under direct excitation, Cl-HABI cleaves from the first excited singlet state into two identical lophyl radicals (L$^{\bullet}$). These radicals lead to hydrogen abstraction from a hydrogen donor (amine or thiol), and produce two initiating radicals. [14] As this compound exhibits a very limited absorption band in the UV, one can take advantage from its high capability to be sensitized by visible light photosensitizers (PS). In the sensitized reaction, the mechanism was proved to be a photoinduced electron transfer from the excited PS to the ClHABI ground state. The corresponding Cl-HABI anion radical is very efficiently cleaved to a lophyl radical (L$^{\bullet}$) and an lophine anion (L^{-}). The latter (L^{-}) give rise immediately to a back electron transfer to the sensitizer radical cation (PS$^{\bullet+}$), leading to an additional lophyl radical (L$^{\bullet}$). Therefore, the dye is completely recovered during process, and one absorbed photon yield to the formation of two lophyl radicals, and then two initiating radicals.[15-17]

Turning back to the dye / hydrogen donors, it was found for some time that certain additives improve the polymerization efficiency. The mechanism involved is not always clear but it is assumed that different radical intermediates generated during the irradiation and in the subsequent polymerization reaction, react with the additive to give new initiating radicals. Three kinds of such additives can be considered:

i) those that form active species from latent species of low reactivity. Molecules having S-H, P-H, Si-H or Ge-H bonds can act as chain transfer agents. These compounds generally form radicals by donating hydrogen to radicals having low reactivity or undergoing oxidization and subsequent deprotonation. One of the mostly used compound is the 2-mercaptobenzimidazole.

ii) molecules that form active species when oxidized. Alkylate complexes such as triarylalkyl borates, alkyl amines such as ethanolamines, N-phenylglycines, N-phenyl-iminoacetic acid and N-trimethylsilylmethyl anilines, sulfur- or tin- containing compounds, sulfinates such as sodium aryl sulfinates are additives exhibiting low oxidation potentials.

iii) molecules that are able to give active species when reduced are characterized by low reduction potentials. Triazines exhibit high reduction potential and lead to carbon-chlorine cleavage. Oxygen peroxides, iodoniums, sulfoniums, pyridiniums, iron arene complexes, and hexaarylbisimidazole derivatives react through such process. [1-4, 10-12]

4. Pyrromethene dyes in three-component photoinitiating systems

Pyrromethene dyes have been rarely used in photoinitiating systems for free radical photopolymerization. [18-19] Recently, the efficiency of these dyes has been outlined in three-component systems based on photoinduced electron transfer process. [20]

4.1. Photopolymerization reaction

Table 1 shows the composition of the different runs performed using EMP as photosensitizer.

Figure 1 shows the kinetics of photo-polymerization obtained for the different formulations under an intensity of 10 mW/cm^2 at 532 nm, and Table 2 collects the corresponding inhibition times t_{inh}, maximum rates of polymerization Rp_{max} and final conversion C_{max}.

Table 1. Composition of the different runs in weight percentages.

Run	NPG (%wt)	TA (%wt)	Molar ratio Donor/Acceptor
1	1.8	**	
2	**	1%	
3	1.8	1%	5/1
4	0.36	5%	1/5
5	0.72	2%	1/1

It is found that EMP alone is not able to perform the conversion of the monomer. In the presence of NPG (Run 1), a low rate of polymerization and a low final conversion are noted, showing that pyromethene dyes are not able to react through hydrogen transfer reaction with NPG.

The system EMP/TA is by far more efficient, and a final conversion of 52 % is noted with a good rate of polymerization.

Table 2. Inhibition times t_{inh}, maximum rates of polymerization Rp_{max} and final conversion C_{max} (intensity 10 mW/cm² at 532 nm).

Run	t_{inh}(s)	Rp_{max}	C_{max}(%)
EMP1	n.m.	n.m.	7
EMP2	7.1	1.1	52
EMP3	1.6	2.6	74
EMP4	1.3	4.7	78
EMP5	2.1	3.5	76

n.m.: not measurable.

The addition of an electron acceptor to the system EMP / NPG makes the photopolymerization much more efficient. Both the rates of polymerization and the final conversions increase noticeably (Runs 3 to 5). The behaviour of the three-component photoinitiating system EMP / NPG / TA clearly underlines a beneficial effect when compared to the separate behaviour of the EMP / NPG and EMP / TA systems.

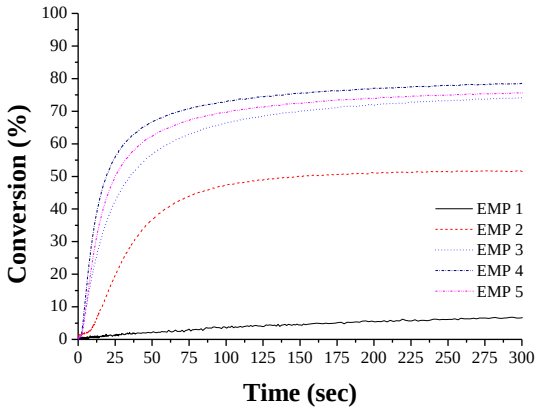

Figure 1. Photopolymerization of SR 349 using EMP as photosensitizer, NPG as electron donor and TA as electron acceptor (intensity 10 mW/cm² at 532 nm).

Comparison of Runs 3 to 4 shows that the most important rate of polymerization is found when the molar ratio TA/NPG is high, a fact that may be related to the photochemical processes involved.

4.2 Mechanism of interaction

In order to get more insights into the photochemical processes that take place during the irradiation of the photoinitiating system, the photochemical interactions between the dye and the coinitiators were investigated through fluorescence spectroscopy. EMP is indeed known to exhibit a high fluorescence quantum yield (ϕ_f = 0.85 in acetonitrile [21], and the photoreactivity of this dye is expected to occur predominantly from the first excited singlet state ^{1}EMP.

Figure 2 shows the fluorescence spectrum of EMP in acetonitrile in the presence of increasing amounts of TA. The corresponding rate constant of quenching k_q can be calculated from the decrease of the fluorescence intensity by using the Stern-Volmer equation.

$$\frac{I_0}{I} = 1 + k_q \tau_0 [Q] \qquad (2)$$

where I_0 and I are the fluorescence intensities in the absence and in the presence of quencher Q, respectively, and τ_0 is the fluorescence lifetime of EMP (6.8 ns [22]). Accordingly, TA leads to a rate constant of $k_q^{TA} = 1.3\ 10^{10}\ M^{-1}s^{-1}$, a value close to the diffusion limit in acetonitrile ($2.0\ 10^{10}\ M^{-1}s^{-1}$).

In the case of NPG as quencher, the quenching rate constant is $5.5\ 10^{9}\ M^{-1}s^{-1}$. As can be seen, NPG is less efficient than TA as quencher, explaining the lower reactivity of NPG compared to TA (cf Runs 1 and 2).

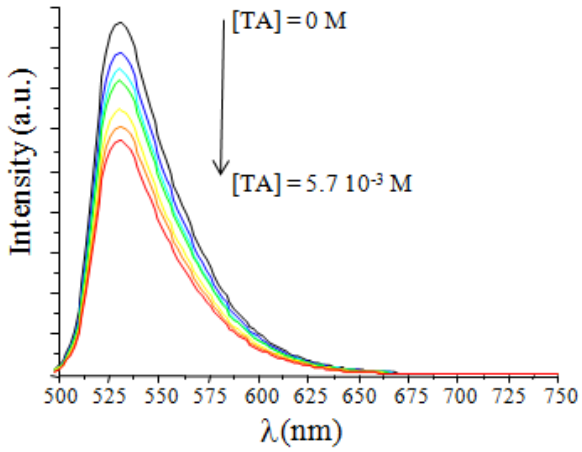

Figure 2. Fluorescence spectrum of EMP in acetonitrile quenched by the addition of TA (excitation at 494 nm).

From these results, one can anticipate an electron transfer reaction from NPG to ^{1}EMP, leading to the formation of the radical anion of the dye $EMP^{\bullet -}$ and the radical cation of the amine $NPG^{\bullet +}$. The later radical cation should further deprotonate to yield the initiating radical $NPG_{-H}^{\bullet}$:

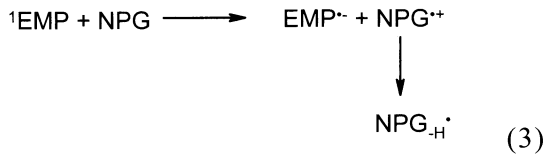

(3)

In the case of TA, an electron transfer takes place from ^{1}EMP to TA, leading to the radical cation of the dye and the radical anion of TA. The later species leads to a fast cleavage, and the formation of initiating radical:

(4)

When both coinitiators are present, a clear beneficial effect is noted, due to secondary reactions that take place between $EMP^{\bullet -}$ and TA. As the quenching rate constant of TA with ^{1}EMP is higher than the one of NPG, TA is expected to react first (at a molar ratio NPG/TA of 1):

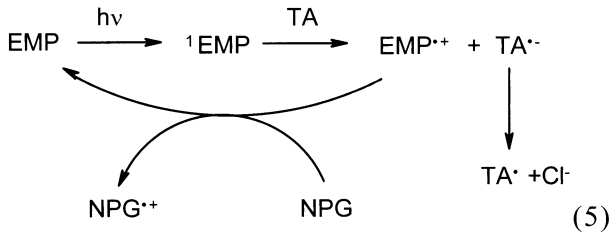

(5)

This leads to both the recovery of the starting dye and an additional formation of initiating radical.

3.3 Formation of the polymeric network

Interesting information about the termination reaction which occur during the curing process can be obtained from the study of the photopolymerization under different intensity of light. Classically, free radical photopolymerization is described in three steps: initiation, propagation and termination [23-25]. The first one (initiation), is the photolysis of initiator system PIS to give primary radicals $R^{\bullet}$. $R^{\bullet}$ reacts with the monomer M, forming a first macroradical $RM^{\bullet}$. The second step is the propagation of the polymerization; the active monomers react with monomers to form a growing polymer chain $RM_n^{\bullet}$ (or a crosslinked three dimensional polymer chains in the case of multifunctional monomer groups). The last step is the termination where the active polymer chains are stopped either by bimolecular recombination of two growing chains or by first order radical trapping termination in the solid environment [23, 26-27]. The network formation by radical-free polymerization of multifunctional monomers induces dramatic changes in the mobility of monomers and polymer chains, leading to the specific autoacceleration (Trommsdorff effect where termination is diffusion controlled while propagation is not) [23, 27-28] and autodecelaration processes (where propagation begins also to be diffusion controlled) [23, 26-27]. Moreover the termination was supposed to start by bimolecular reaction at low conversion degree and ends, as the reaction medium is freezed by the network, mainly by radical trapping at high conversion degree [23, 26-27]. However it is been shown [29-34] that termination mechanisms occur by reaction-diffusion, where two or more growing chains can recombine by chain propagation even if the mass center of growing polymer chains are frozen in the glassy network: the so called reaction diffusion termination.

The reaction-diffusion takes place from low conversion degree, less than around 10%, until very high conversion. [35] At this stage the termination rate coefficient is somehow constant, low and proportional to the propagation rate coefficient [30, 35]. At very high conversion, where monomer diffusion is also stopped, termination becomes mainly governed by monomolecular radical trapping [23, 26-27, 36]. A possible approach for the estimation of the relative contributions of monomolecular or bimolecular termination is based on the light intensity exponent α in the expression for the polymerization rate below [23, 37]:

$$Rp = k(C(\%))[M]I_0^{\alpha} \qquad (6)$$

where k is a conversion-dependent quantity, I_0 is the incident light intensity. Under real conditions α is often found different of 0.5. Reasons for this could be gel effect, radical transfer reactions, and primary radical termination [34]. Thus the following values for α are possible:

- $\alpha = 1$: first-order (radical trapping) or pseudo first-order termination;
- $0.5 < \alpha < 1$: combined first- and second-order termination;
- $\alpha = 0.5$: second-order termination (bimolecular recombination);
- $\beta < 0.5$: primary radical termination.

In the case of purely bimolecular termination, one should observe the square root dependence on the absorbed light intensity, and in the case of purely monomolecular termination the first order dependence.

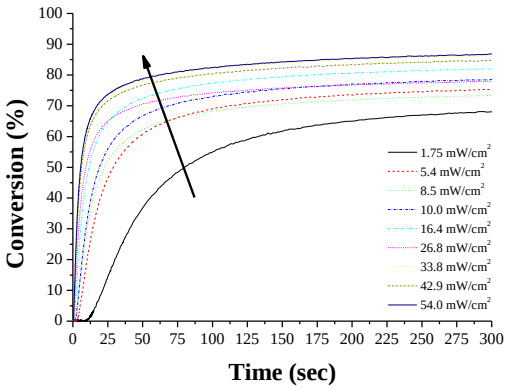

Figure 3. Photopolymerization of SR 349 with Run 4 formulation (molar ratio donor/acceptor of 1/5) at different light power.

Therefore, varying the light intensity allows the study of termination processes and could give some information about the formation of the polymer network during the polymerization process.

Figure 3 shows the conversion curves at different intensity of light. Obviously, the rate of polymerization and the final conversion increase when the intensity increases, while the inhibition time decreases.

Figure 4 shows the polymerization rates Rp vs. conversion C(%) curves at different light power. According to the model of multifunctional monomers polymerization one can see that the autoacceleration region, in which termination is diffusion controlled but propagation has not begun at very short conversion values, the maximum polymerization rate being reached at around 10% conversion for all the values of the light power. Then the autodeceleration region is observed where both termination and propagation are diffusion limited.

From the values of Rp at a given conversion it is possible to determine the α exponent of I_0 at the different conversion degrees. The plot of Ln(Rp) as a function of Ln(I_0) from 5 to 40 % conversion are given in the Figure 5, together with their corresponding linear regression. α values are

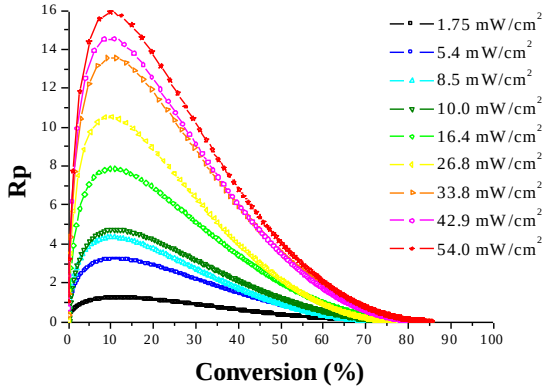

Figure 4. Evolution of SR349 polymerization rate Rp as a function of monomer conversion (Run 4 with donor/acceptor ratio of 1/5).

obtained by the slope of the linear regression and collected in Table 3.

	5%	10%	15%	20%	25%	30%	35%	40%
α	0.78	0.77	0.76	0.75	0.75	0.74	0.75	0.75

Table 3. α values obtained for Run 4 at different degrees of conversion.

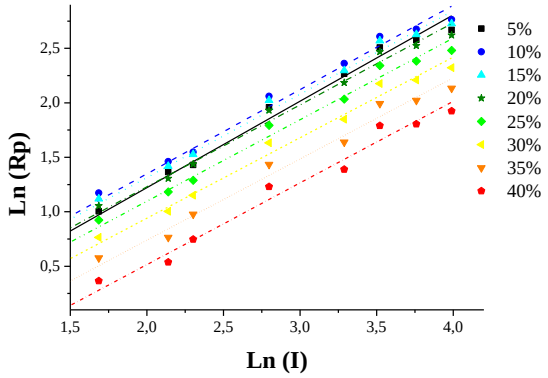

Figure 5. Determination of the the light intensity exponent α in photopolymerization of SR 349 with Run 4 (molar ratio donor/acceptor of 1/5).

As can be seen from Table 3, the α value is almost constant during the curing process, with variations from 0.78 at 5% conversion decreasing to 0.75 at 40%. This indicates that the termination involves mixed processes with both monomolecular (radical trapping) and bimolecular (reaction-diffusion) reactions.

5. Conclusion

In this paper, the ability of a three-component photoinitiating system based on a pyrromethene dye to initiate the photopolymerization of acrylates was investigated. The mechanism is studied through fluorescence spectroscopy, and this helps to understand the role of the different components. After a primary photoinduced electron transfer, the ion radical of the dye react with a redox additive to yield the recovery of the starting dye and an additional initiating radical. The effect of the relative concentration of the coinitiators is clearly evidenced.

References

1. J.P. Fouassier, "*Photoinitiation Photopolymerization and Photocuring*", Hanser Publishers, Munich, New York, (1995).
2. "*Photochemistry and UV curing: New trends*", J.P. Fouassier Ed., Research Signpost, Trivandrum, 2006.
3. X. Allonas, C. Croutxe-Barghorn, J.P. Fouassier, J. Lalevée, J.P. Maleval, F. Morlet-Savary, in "*Lasers in Chemistry, Vol2. Influencing Matter*", M. Lackner Ed., Chap. 35, Wiley, (2008).
4. J.P. Fouassier, X. Allonas, J. Lalevée, in *"Macromolecular engineering: from precise macromolecular synthesis to macroscopic materials properties and applications"*, K. Matyjaszewski, Y. Gnanou, L. Leibler, Eds, vol 1, 643-672, Wiley-VCH, Weinheim, 2007.
5. J.P. Fouassier, X. Allonas, D. Burget, *Prog. Org. Coat.*, **47** (2003) 16-36.
6. C. Decker, K. Moussa, *Macromolecules* **22** (1989) 4455.
7. X. Allonas, C. Grotzinger, J. Lalevee, J.P. Fouassier, M. Visconti, *Eur. Polym. J.*, **37** (2001) 897.
8. X. Allonas, J.P. Fouassier, L. Angiolini, D. Caretti, *Helv. Chim. Acta* **84** (2001) 2577.
9. C. Dietlin, X. Allonas, A. Defoin, J.P. Fouassier, *Photochem. Photobiol. Sci.*, **7** (2008) 558.
10. G. Oster, N.L. Yang, *Chem. Rev.*, **68** (1968) 125.
11. B.M. Monroe, G.C. Weed, *Chem. Rev.*, **93** (1993) 435
12. C.G. Roffey, "*Photogeneration of reactive species for UV curing*", John Wiley & Sons, Chichester, (1997).
13. G.R. Coraor, R.H. Riem, A. MacLachlan, E.J. Urban, *J. Org. Chem.*, **36** (1971) 2272
14. D.F. Eaton, A.G. Horgan, J.P. Horgan, *J. Photochem. Photobiol., A*, **58** (1991) 373.
15. Q.Q. Zhu, M. Fink, F. Seitz, S. Schneider, W. Schnabel, *J. Photochem. Photobiol., A*, **59** (1991) 255.
16. X. Allonas, J.P. Fouassier, M. Kaji, M. Miyasaka, T. Hidaka, *Polymer*, **42** (2001) 7627.
17. X. Allonas, JP. Fouassier, M. Kaji, Y. Murakami, *Photochem. Photobiol. Sci.*, **2** (2003) 224.
18. S. Blaya, P. Acebal, L. Carretero, A. Fimia, *Opt. Com.*, **228** (2003) 55.
19. O. Garcia, A. Costela, I. Garcia-Moreno, R. Sastre, *Macromol. Chem. Phys.*, **204** (2003) 2233.
20. O. Tarzi, X. Allonas, C. Ley, J.P. Fouassier, *J. Polym. Sci., Part A: Polym. Chem.*, under press
21. G. Jones, S. Kumar, O. Klueva, D. Pacheco, *J. Phys. Chem. A*, **107** (2003) 8429.
22. Suzuki, S.; Allonas, X.; Fouassier, J. P.; Urano, T.; Takahara, S.; Yamaoka, T. *J. Photochem. Photobiol. A: Chem.*, **181** (2006) 181.
23. E. Andrzejewska, *Prog. Polym. Sci.*, **26** (2001) 605.
24. D. L. Kurdikar, N. A. Peppas, *Macromolecules*, **27** (1994) 4084.
25. C.N. Bowman, N. A. Peppas, *Macromolecules* **24** (1991) 1914.
26. S. Zhu, Y. Tian, A. E. Hamielec, D.R. Eaton, M*acromolecules*, **23** (1990) 1144
27 M. Wen, A. V. McCormik, *Macromolecules,* **33** (2000) 9247.
28 T.J. Tulig, M. Tirell, *Macromolecules*, **14** (1981) 1501.
29. K. S. Anseth, C. N. Bowman, *Polym. React. Eng.*, **1** (1993) 499.
30. K. S. Anseth, C. M. Wang, C. N. Bowman, *Macromolecules*, **27** (1994) 650.
31. K. S. Anseth, L.M. Kline, T.A. Walker, K.J. Anderson, C.N. Bowman, *Macromolecules* **28** (1995) 2491.
32. K.S. Anseth, C. Decker, C. N. Bowman, *Macromolecules*, **28** (1995) 4040.
33. M. D. Goodner, H. R. Lee, C. N. Bowman,

Ind. Eng. Chem. Res., **27** (1997) 1247.
34. M. D. Goodner, C. N. Bowman, *Chem. Eng. Sci.*, **57** (2002) 887.
35. K. S. Anseth, C.N. Bowman, *Polym. React. Eng.*, **1** (1993) 499.
36. T. M. Lovestead, J. A. Burdick, K. S. Anseth, C. N. Bowman, *Polymer,* **46** (2005) 6226.
37. C. Decker, H. Kaczmarek, *J. Appl. Polym. Sci.*, **54** (1994) 2147.